

AIAA-2010-0162

Generation of conjugate meshes for complex geometries for coupled multi-physics simulations

WN Dawes,*

CFD Laboratory, Department of Engineering, University of Cambridge, Cambridge CB2 1PZ, UK,
and

WP Kellar & SA Harvey,
Cambridge Flow Solutions Ltd, Compass House, Vision Park, Cambridge, CB24 9AD, UK

Over recent years we have developed and published research aimed at producing a meshing, geometry editing and simulation system capable of handling large scale, real world applications and implemented in an end-to-end parallel, scalable manner. The particular focus of this paper is the extension of this meshing system to include conjugate meshes for multi-physics simulations. Two contrasting applications are presented: export of a body-conformal mesh to drive a commercial, third-party simulation system; and direct use of the cut-Cartesian octree mesh with a single, integrated, close-coupled multi-physics simulation system.

I. Introduction

In the world of aerospace, design requirements are becoming ever more demanding and as simulation software becomes ever more reliable there is a trend towards automated design optimization. This naturally leads to the need to link more disciplines together. For example as soon as an aero-thermal simulation can be performed for a cooled turbine blade the urge becomes imperative to couple in FE analysis on the metal side to predict hot-cold running geometries or perhaps to estimate blade life. Casting simulations can be performed to check on blade manufacturability...and so on. The overarching imperative is to gather all of this together in integrated “process chains” for routine industrial exploitation – leading towards automated design optimization. Some impressive papers are starting to be published in this area. For example, Amaral et al [2008] and Verstaete et al [2008] show air and metal-side meshes coupled together to perform conjugate flow, thermal and stress simulations with a focus on optimizing blade life.

At the core of this activity is geometry and mesh generation. The geometries can be very complex – in many cases with arbitrary topology. The need to generate large meshes in a scripted and guaranteed manner as the geometry is edited is a critical enabling requirement for any automated optimization. Our work has had a strong focus in this area for a number of years (see Dawes *et al* [2005-2009]) and in particular a recent publication, Dawes *et al* [2009] shows a first application of our work to a very simple topological optimization study of a cooled turbine blade.

The purpose of this paper is to show extensions of our mesh generation and geometry editing system to include conjugate meshes to support multi-physics simulations. Two contrasting applications are presented: export of a body-conformal mesh to drive a commercial, third-party simulation system; and direct use of the cut-Cartesian octree mesh with our own single, integrated, close-coupled multi-physics simulation system.

* wnd@eng.cam.ac.uk

II. BOXER: parallel, bottom-up octree mesh generation

The BOXER software system represents an attempt to integrate the whole CFD Process “end-to-end” from CAD import through mesh generation, flow solution & post-processing - including the ability to edit the geometry. BOXER has been implemented, at least to prototype standard, end-to-end in parallel—including all data flows between functional units. BOXER was inspired by exploration of the possibilities offered by the integration of the solid modeling directly with the mesh generation & with the flow solution—this combined ideas from solid modeling (see for example Samareh [1999] & Haines *et al* [1998]) with virtual sculpting (see for example, Galyean *et al* [1991], Perng *et al* [2001] and Baeretzen [2001]) combined in the context of a simple, cut-Cartesian mesh flow solver (see Viecegli [1971], Bussoletti *et al* [1985] or Aftosmis *et al* [1998]). The evolution of the software has been described in a series of linked publications. Dawes *et al* [2005]) first gathered together and set out these building blocks and showed their potential as a rapid prototyping design tool. Then Dawes *et al* [2006, 2009] showed how these building blocks could be efficiently implemented in parallel. The cut-cell issue was addressed in Dawes *et al* [2007] showing how layer meshes and/or body-conformal meshes could be exported.

The backbone of BOXER is a very efficient octree data-structure acting *simultaneously* as a search engine, as a spatial occupancy solid model and as an adaptive, unstructured mesh for the flow solver. This provides unlimited geometric flexibility and very robust mesh generation. The solid model is initialised by the import of a tessellated surface from a variety of potential sources (most CAD engines have an STL export) or by direct interrogation of the CAD solid model kernel itself (Haines *et al* [1998]). The solid model is captured on the adaptive, unstructured Cartesian hexahedral mesh very efficiently by cutting the tessellated boundaries using basic computer graphics constructs developed for interactive 3D gaming. This geometry capture is very fast; for example, a body represented by about 1M surface triangles can be imported into a mesh of around 11M cells (with 6-7 levels of refinement) in approximately 2 minutes on a single, top-end PC—very much faster in parallel. The spatial occupancy solid model is sampled as a distance field and managed as a Level Set; this forms a solid modeling kernel to support all the activities of the code. Adaptive mesh refine/de-refine for the flow and for the geometry, via the distance field, enables both moving bodies and topology editing.

III. Generation of conjugate meshes

The generation of conjugate meshes follows on naturally from the background cut-Cartesian octree approach. As illustrated in Figure 1, the air-side and metal-side meshes emerge simultaneously as the tessellated geometry is cut into the octree and with little cost extra overhead to manage and maintain both meshes.

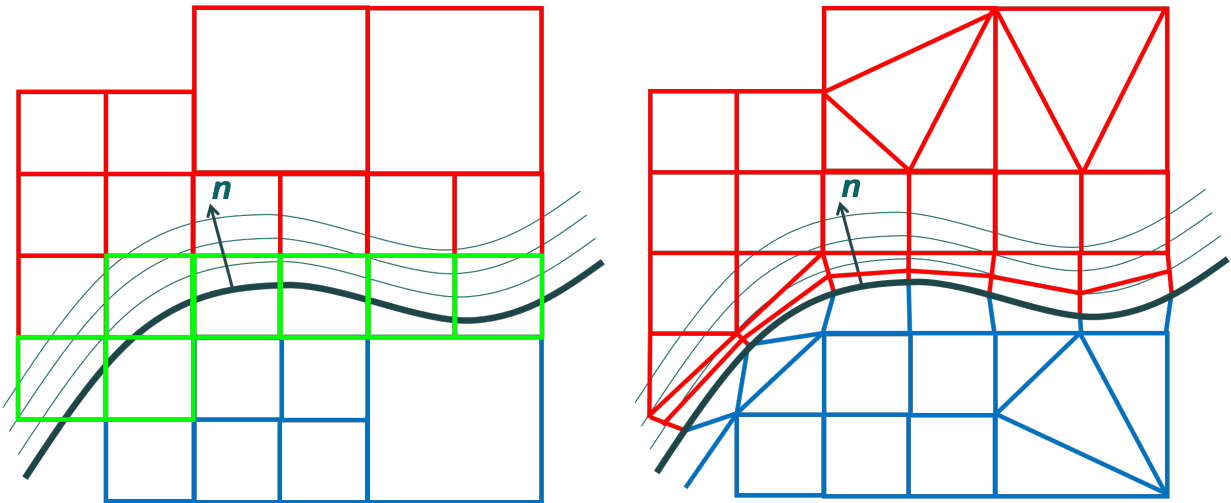


Fig.1: Schematic of conjugate octree mesh generation: (left) cut-Cartesian form; (right) body-conformal

The conjugate cut-Cartesian meshes can be used as they are with appropriate solvers (for flow, thermals, stress etc.) which have cut-cell capability; indeed, extensions to the BOXER solver to permit integrated simulation of conjugate flow/thermal/elastic stress on such meshes will be described later in this paper.

It is also advantageous to derive a body-conformal mesh export to drive third party commercial simulation systems. Our basic approach, as described in Dawes *et al* [2007], and sketched in Figure 1 (right), is to manipulate the mesh near the geometry surfaces so that a body-conformal mesh can be exported – with layer mesh insertion if required. This near-wall mesh “manipulation” uses a mixture of shape-insertion (like Yerry *et al* [1983]) and automated mesh quality optimization to produce a guaranteed quality mesh (see also Dawes *et al* [2009]). This approach can be trivially applied to the metal-side mesh as well as on the air-side. However, the resulting mesh will not necessarily be continuous from metal to air-side and this may give the target simulation system some difficulties on very complex geometries as the simulation system has to perform repeated air-to-metal-to-air side interpolations. Hence, currently we can also export meshes that are continuous across the air-metal interface. To achieve this, an additional optimization loop needs to be added to maintain mesh quality across the air-metal interface.

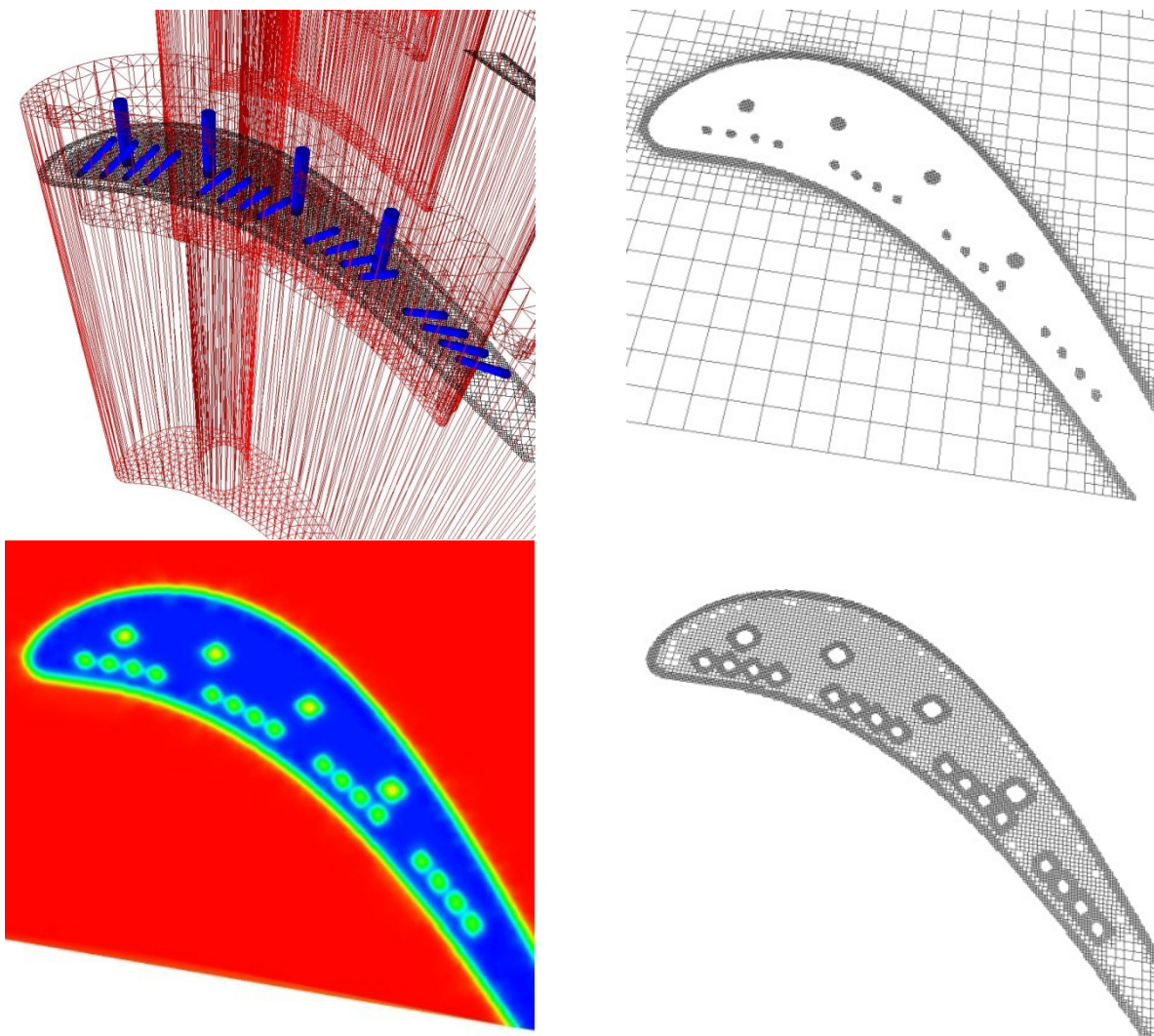


Figure 2a: Tessellated input with virtual tools for a cooled turbine geometry (top); (bottom) distance field (red=airside, blue=metal-side)

Figure 2b: The basic cut-Cartesian octree mesh: top is the air-side and bottom the metal-side.

As a practical illustration, Figure 2a shows the tessellated (STL) input for a cooled turbine geometry (Janke *et al* [2008]) together with some virtual tools (see Dawes *et al* [2005]); the tools cut the suction side cooling holes and dust holes into the Level Set distance field solid geometry. The distance field is shown red on the airside and blue on the metal-side. Figure 2b shows the basic cut-Cartesian octree mesh: top is the air-side and bottom the metal-side. By contrast, Figure 3 shows the solid model, surface mesh and conjugate mesh for a generic, cooled automotive brake assembly exported in body-conformal form.

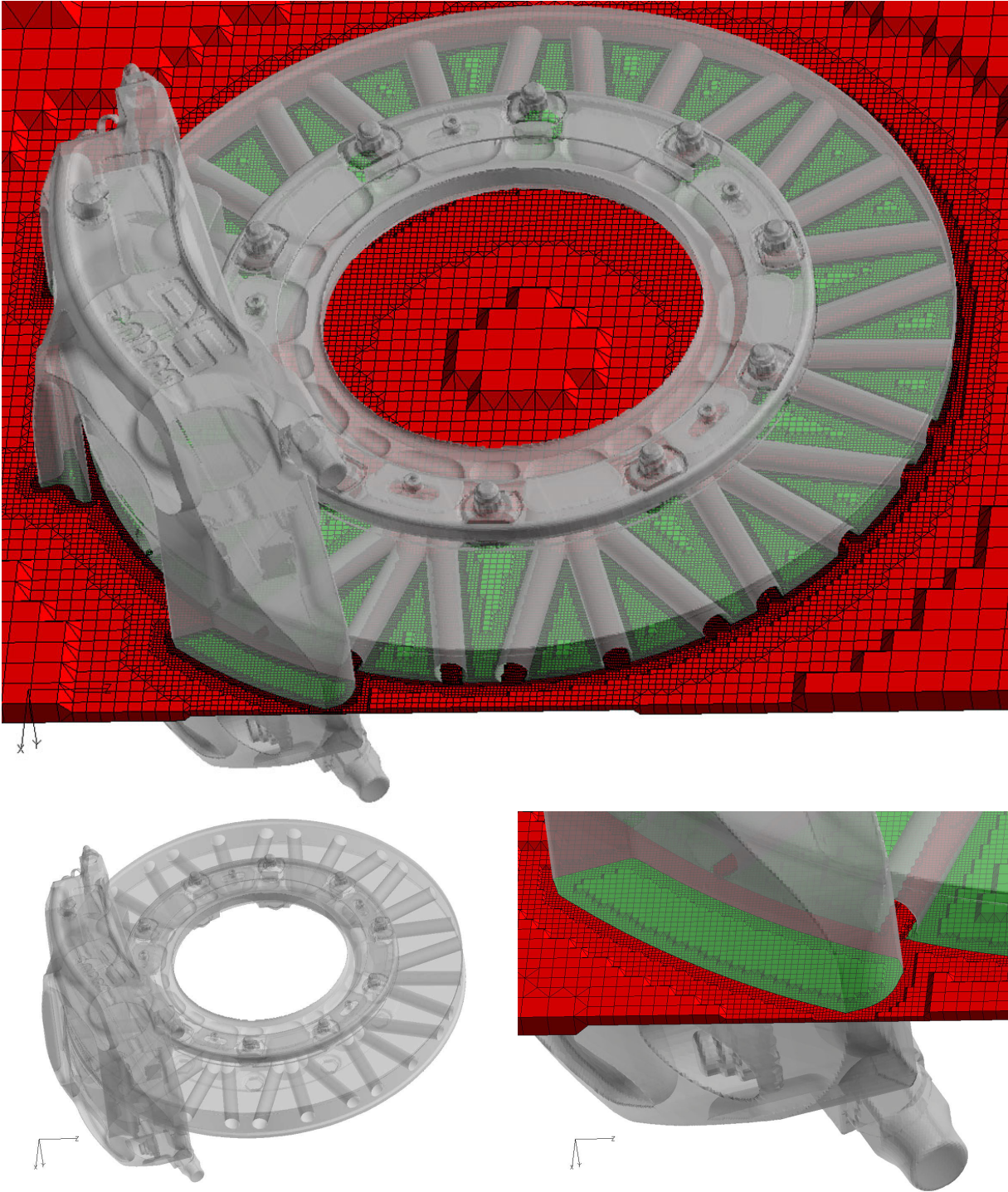


Fig.3: Solid model, surface mesh and conjugate mesh for a generic, cooled automotive brake assembly.

IV. Application 1: export of a body-conformal mesh to drive a commercial, third-party simulation system

As a practical demonstration we show an example of a simple simulation with body-conformal conjugate meshes. The case is the classic set up of an inclined cooling hole discharging into a free stream. Figure 3 shows BOXER conjugate meshes for the air-side (top left and middle) and the metal-side (bottom left and middle) with FLUENT conjugate aero-thermal simulations (showing the temperature field) performed on the exported BOXER mesh. These meshes were non-continuous across the air-metal interface and FLUENT was able successfully to interpolate, via an implicit heat transfer coefficient, between the coupled aero and thermal simulations.

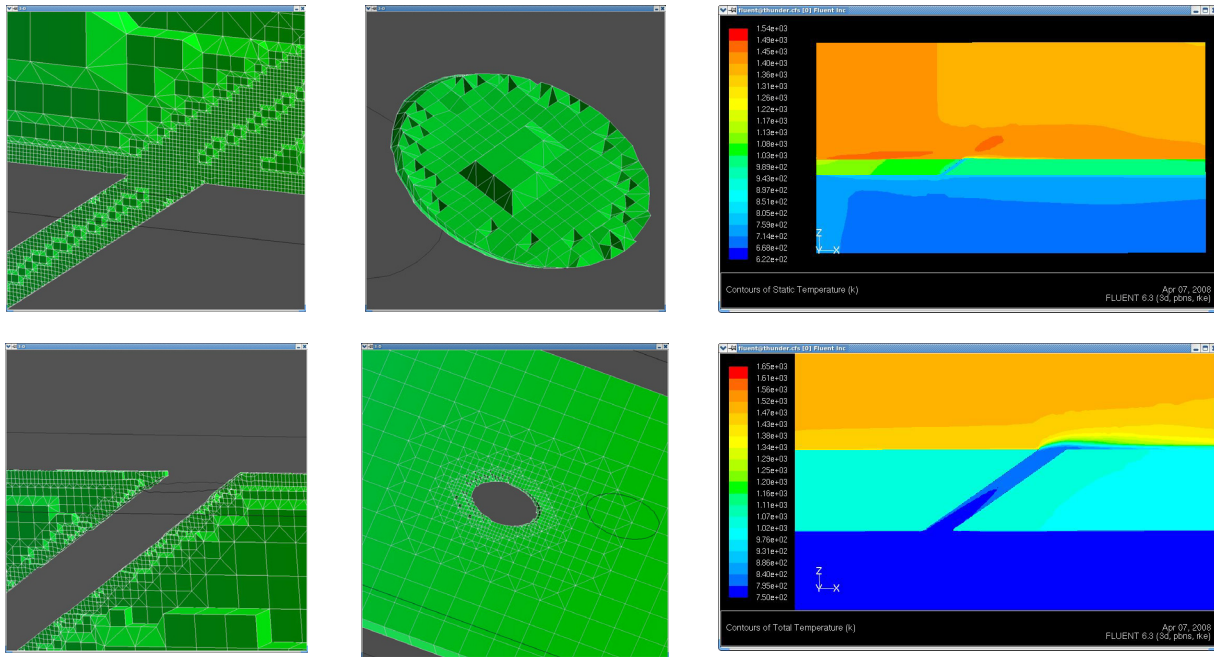


Fig.4: BOXER conjugate meshes for the air-side (top left and middle) and the metal-side (bottom left and middle) with FLUENT conjugate aero-thermal simulations (temperature field).

V. Application 2: direct use of the cut-Cartesian octree mesh with a single, integrated, close-coupled multi-physics simulation system

Rather than use third-party simulation systems, probably scripted together and very likely communicating data via a serial bottleneck, there are attractions to exploring a unified, integrated, multi-physics approach (see for example Davison *et al* [2008] and Dulikravich *et al* [2001]). In the following sections the development within the BOXER solver framework of air-side and then conjugate metal-side thermal and elastic stress simulations will be described.

The air-side flow solver

The basic solver is based on earlier work on unstructured meshes (the NEWT code – see Dawes [1993]) and can be summarised as:

- second order finite volume

- time marching (Adams-Bashforth or Runge-Kutta)
- simple mixing length turbulence model
- low-Mach number preconditioning
- optional agglomeration multi-grid

The basic algorithm was generalised to permit h-2h mesh transitions to be handled. Special boundary conditions were added for the cut cells which are treated via ghost cells combined with local body normals (derived from the distance field) allowing the full shape and curvature of the body to be respected. Classical wall functions (see Launder [2007]) are then used to fill these ghost cells.

The conjugate heat transfer solver

On the metal side the classic heat transfer conduction equation is:

$$\rho c_p \frac{\partial T}{\partial t} = -\lambda \nabla^2 T$$

This can be readily discretised in finite volume form on the conjugate, cut-Cartesian mesh and solved with simple, explicit time-marching (with the option of agglomeration multi-grid):

$$T^{n+1} = T^n - \Delta t \frac{\lambda}{\rho c_p} \nabla^2 T^n$$

This can be trivially implemented in parallel and uses very little additional computer storage compared to the flow solver.

The key aspects of the conjugate heat transfer solution are the air-metal boundary conditions and their coupling. Figure 5 sketches the approach used. The cut cells are handled via a ghost method with the local wall normal ensuring a body-aligned flow and, in conjunction with the first off-wall flow cell, supporting a classical wall function (see for example Launder [2007]) for both the skin friction and wall heat transfer. This use of wall functions is certainly a weakness of the present approach and will be improved in future work. Provision can also be made for Thermal Barrier Coating (TBC) via an additional heat transfer coefficient. Following Divo *et al* [2003] the temperature fields on the air-side, in the ghost cell and on the metal side are updated simultaneously with the wall heat flux acting as the coupling link. Convergence can be enhanced by having an inner loop for the conjugate cells performing 10-100 metal-side iterations for every air-side iteration (see Figure 6).

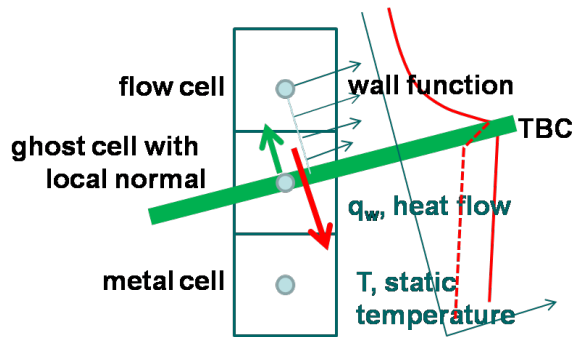


Fig.5: The air-metal boundary conditions for CHT

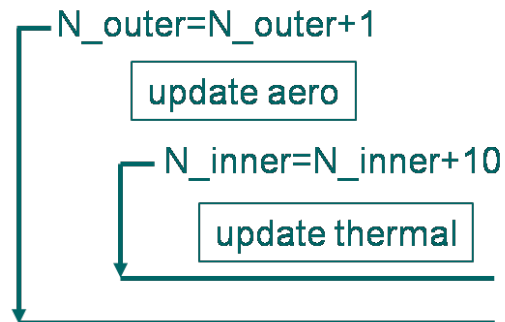


Fig.6: The outer/inner iteration strategy

The conjugate elastic stress solver

Overview

Also on the metal-side, the elastic stress equations can be discretised and solved. The classical equations for linear, homogeneous, isotropic elasticity are well known (see for example Legace [2002]) and are as follows.

Stress and strain are related by Hooke's law:

$$\boldsymbol{\sigma} = [\mathbf{C}]\boldsymbol{\varepsilon}$$

where:

$$[\mathbf{C}]^{-1} = \begin{bmatrix} 1/E & -\nu/E & -\nu/E & 0 & 0 & 0 \\ -\nu/E & 1/E & -\nu/E & 0 & 0 & 0 \\ -\nu/E & -\nu/E & 1/E & 0 & 0 & 0 \\ 0 & 0 & 0 & 1/\mu & 0 & 0 \\ 0 & 0 & 0 & 0 & 1/\mu & 0 \\ 0 & 0 & 0 & 0 & 0 & 1/\mu \end{bmatrix}$$

with E Young's modulus and ν Poissons ratio. The strain tensor $\boldsymbol{\varepsilon}$ is defined in terms of the material displacement \mathbf{u} by:

$$\varepsilon_{ij} = \frac{1}{2} \left(\frac{\partial u_i}{\partial x_j} + \frac{\partial u_j}{\partial x_i} \right)$$

and the stress tensor is defined by:

$$\sigma_{ij} = \lambda \varepsilon_{kk} \delta_{ij} + 2\mu \varepsilon_{ij} - 3\alpha\kappa(T - T_{ref})\delta_{ij}$$

where the Lamé constants are:

$$\mu = \frac{E}{2(1+\nu)}; \lambda = \frac{E\nu}{(1+\nu)(1-2\nu)}$$

The last term in the stress tensor represents the thermal stresses with T_{ref} a reference temperature, κ the bulk modulus and α the coefficient of thermal expansivity.

A basic force balance in the presence of external force \mathbf{f} leads to the classic elasticity equation to be solved in the presence of appropriate boundary conditions (on a combination of \mathbf{u} and $\boldsymbol{\sigma}$):

$$\rho \frac{\partial^2 \mathbf{u}}{\partial t^2} + \text{div } \boldsymbol{\sigma} + \mathbf{f} = \mathbf{0}$$

Traditionally this is discretised using a Finite Element methodology leading to the need to solve a large, sparse matrix problem: $[\mathbf{A}]\mathbf{u}=\mathbf{b}$. However, this requires a large amount of computer memory – orders of magnitude more than that consumed by a typical flow solver on the same mesh – and can inhibit parallel implementation. This severely restricts the problem size which can be efficiently handled. Whilst there are now sparse matrix solvers implemented in parallel, for example Adams *et al* [2004] (which shows structural analysis on meshes with up to 500M DOF on cpu clusters with ~4000 cores in under an hour), it would seem more natural to solve the elasticity equation iteratively (as suggested in Davison *et al* [2008] for example).

Accordingly, in the present work the elasticity equation is discretised in a rather straightforward finite volume form on a cut-Cartesian mesh and solved using simple time marching:

$$\mathbf{u}^{n+1} = 2\mathbf{u}^n - \mathbf{u}^{n-1} - \Delta t^2 \rho \{\text{div } \boldsymbol{\sigma} + \mathbf{f}\}^n$$

This can be trivially implemented in parallel and uses very little additional computer storage compared to the flow solver. Agglomeration multi-grid can be used to accelerate convergence as well as inner-looping (see Figure 6).

The cut cells are handled in a similar way to the air-side using the local body normal to set appropriate ghost cell values; similar approaches for immersed boundary methodologies can be found in the literature, for example Li *et al* [2004].

Simple validation: beam stresses

As simple validation of this approach the classical problem of the deflection of a simply supported beam was solved. Figure 7 shows a schematic of the case together with a sketch of the very simple discretisation. For the present second order finite volume approach the number of “degrees of freedom” (DOF) equals the number of cells. The next figure, Figure 8 shows the beam centre-line deflection for three different DOF’s made dimensionless with the classical result that the centerline deflection is $(5/384) Wl^3/EI$. As can be seen, as the mesh is refined the analytical result is approached asymptotically.

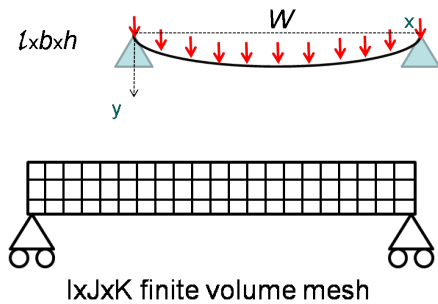


Fig.7: Schematic of the simple beam case: together with the discretisation - DOF, the number of degrees of freedom = $I_x J_x K$

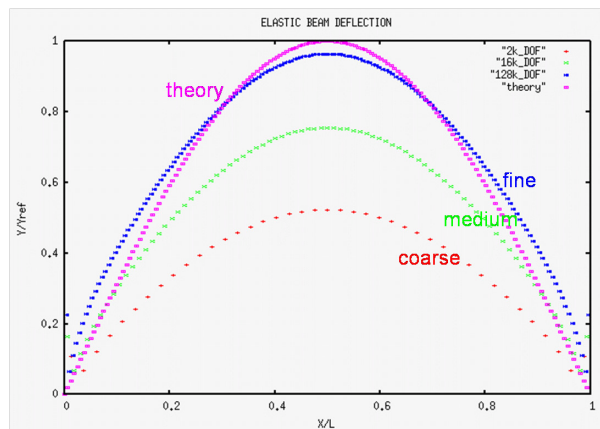


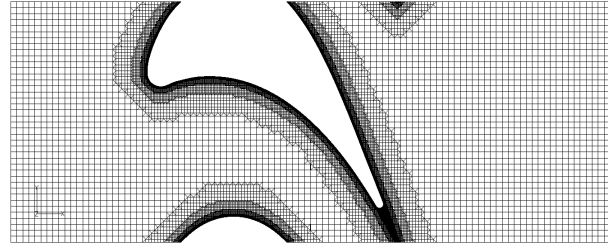
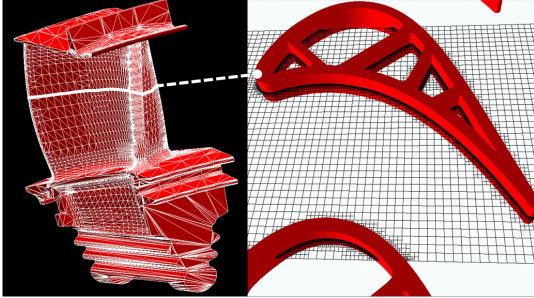
Fig.8: Beam deflection; theoretical result compared to three different mesh sizes

Case study: mid-span section of an HPT rotor blade

The simple case study uses the ACE/RD transonic HPT rotor blade tested in a cascade in the Whittle Laboratory by Haller [1979]. Basic parameters are shown in Figure 9 below.

The first simulation reported in this paper aims to show the basic air-side performance of this rather simple solver (only about 250 lines of code). As well as comparison with data, simulations were performed using FLUENT on the same basic mesh as the BOXER solver but exported in body-conformal form – as described earlier. The basic mesh used for the FLUENT run is shown in Figure 9. Figure 10 compares the BOXER simulations with those from FLUENT in terms of Mach number; Figure 11 makes an entropy comparison; and Figure 12 compares predicted and measured blade surface isentropic Mach numbers. The agreement is felt to be satisfactory.

As basic indication of the air-side thermal performance, Figure 13 shows predicted blade Nusselt number for an uncooled test on the ACE/RD blade compared with data from Abhari *et al* [1992]. The agreement is judged adequate – the main problems are at the LE where the wall function fails to predict the local but large spike and the lack of transition modeling.



Inlet flow angle	56 deg
Exit flow angle	-65 deg
Exit Mach number	0.90
Reynolds number	2.e+05

Basic parameters

Density, ρ	8.22 kg/m**3
Thermal conductivity	80.4 W/mK
Young's modulus, E	208 GPa
Poisson's ratio, ν	0.29
Bulk modulus, κ	208 GPa
Thermal expansivity, α	13.5e-06 /K
TBC, thickness & thermal conductivity	0.8 W/mK 0.3mm

Material properties for Inconel 718 and a typical TBC: ZrO2-Y2O3

Fig.9: The mid-span section of an HPT rotor – the ACE/RD blade

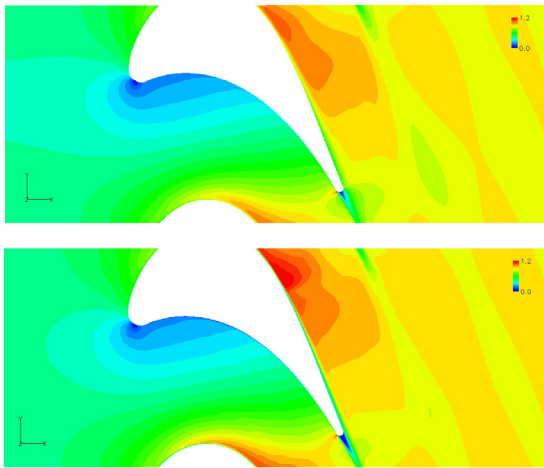


Fig.10: Comparison between BOXER (above) & FLUENT (below): Mach number – range 0 to 1.2

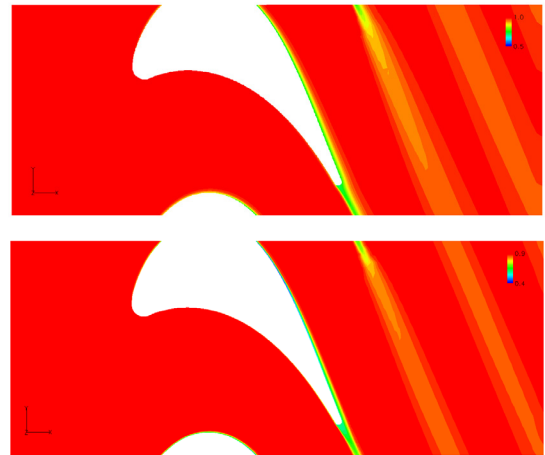


Fig.11: Comparison between BOXER (above) & FLUENT (below) : scaled entropy – range 0.5 to 1.0

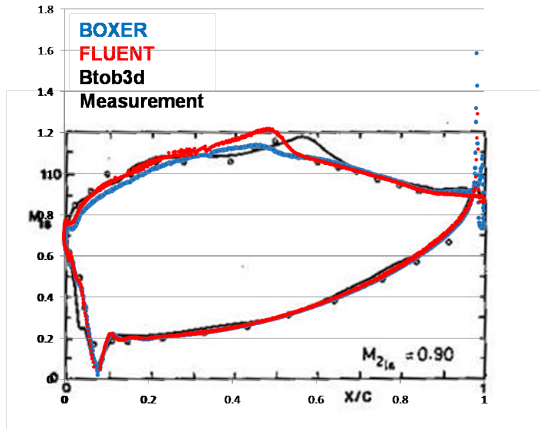


Fig.12: Blade surface isentropic Mach numbers – comparison between data and predictions

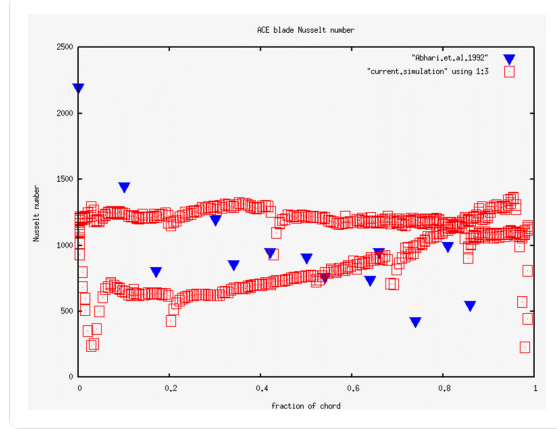


Fig.13: Predicted blade Nusselt number (red) compared with data from Abhari et al [21] (blue)

A 3D but small spanwise section was modeled and spanwise periodic boundary conditions were used for the flow, thermal and stress fields. The primary path boundary conditions and cooling temperature were set to be representative of cruise. A TBC was simulated on the blade surfaces. Inside the cooling passages a correlated heat transfer coefficient was applied – but no passage to passage temperature pick up was specified. The blade was simulated in a cascade – so the free stream total temperature was rather hotter near the blade exit than it would be in a rotor with work extraction. The reference temperature for the thermal stresses was taken as the mean of the free stream stagnation temperature and the cooling temperature and, in fact, the thermal stresses dominate the mechanical. Inconel 718 was selected as a representative blade material and Figure 9 shows the values used for all the material constants.

The results are shown in Figures 14 & 15. Figure 14 shows the metal-side temperature distribution predicted by the Conjugate Heat Transfer simulation and plotted as $(T-T_{cool})/(T_{01}-T_{cool})$ with range 0.16 (blue) to 0.83 (red). The creep life will be clearly limited by excessive metal temperature in the TE region of the blade. What is notable is the very large spatial variability of temperature (and stress as will be seen). An interesting issue is whether the material properties themselves are valid as things like creep life and so on are usually measured under controlled conditions of uniform temperature and background stress. Figure 15 shows the corresponding distribution of the dimensionless von Mises stress, plotted as σ/σ_{max} , and with range 0.1 (blue) to 1.0 (red). In this simulation the stress field is dominated by thermal stresses. It is clear that the fatigue life will be limited by these thermal stresses where the internal cooling passage walls join the main blade wall.

VI. Concluding Remarks & future prospects

This paper has described the extension of the BOXER meshing system to include conjugate meshes for multi-physics simulation. Application to a number of test cases has demonstrated the new capability.

Meshes can be exported in body-conformal form to drive third party simulation systems or can be used in cut-Cartesian octree form with suitable solver software. The extension of the BOXER solver system from aero-alone to conjugate aero, thermal and elastic stress was then described and applied to a simple case study.

Future plans include topological optimization of cooled gas turbine geometries and more formalized life prediction.

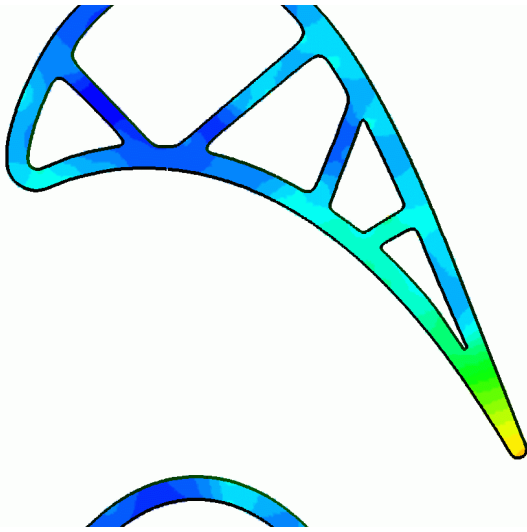


Fig.14: Representative metal-side temperature distribution $(T-T_{cool})/(TOI-T_{cool})$: range 0.16 (blue) to 0.83 (red)

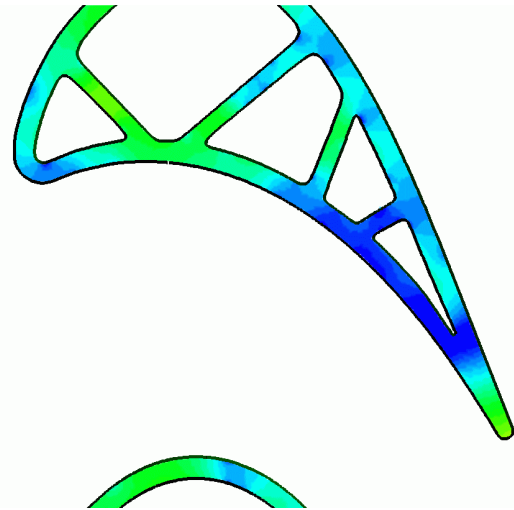


Fig.15: Corresponding distribution of dimensionless von Mises stress σ/σ_{max} : range 0.1 (blue) to 1.0 (red)

VII. References

- Abhari RS, Guenette GR, Epstein AH & Giles MB “Comparison of time-resolved turbine rotor blade heat transfer measurements and numerical calculations” Transactions of the ASME, vol.114, pp.818-, Oct.1992
- Adams MF, Bayraktar HH, Keaveny TM & Papadopoulos P “Ultrascale implicit finite element analysis in solid mechanics with over half a billion degrees of freedom” Super Computing SC’04, Pittsburgh, PA, 2004
- Amaral S, Verstaete T, van dem Braembussche R Arts T “Design and optimization of the internal cooling channels of a HP turbine blade – Part I, Methodology” ASME GT2008-51077, Berlin 2008
- Aftosmis MJ, Berger MJ & Melton JE, “Robust and efficient Cartesian mesh generation for component-based geometry” AIAA J., 36, 6, 952-, 1998
- Arts T, Duboue JM & Rolling G “Aerothermal performance measurement and analysis of a two-dimensional high turning rotor blade” ASME 1987
- Baerentzen A “Volume sculpting: intuitive, interactive 3D shape modelling” IMM, May 2001
- Bussoletti JE, Johnson FT, Bieterman MB, Hilmes CL, Melvin RG, Young DP & Drela M “TRANAIR: solution-adaptive CFD modelling for complex 3D configurations” AIAA Paper 1995-0451, 1985
- Davison JB, Ferguson SE, Mendonca FG & Peck AF “Towards an automated simulation process in combined thermal, flow and stress in turbine blade cooling analyses” ASME Paper GT2008-51287, Berlin, 2008
- Dawes WN “Simulating unsteady turbomachinery flows on unstructured meshes which adapt both in time and space”, ASME Paper 93-GT-104, 1993.
- Dawes WN “Building Blocks Towards VR-Based Flow Sculpting” 43rd AIAA Aerospace Sciences Meeting & Exhibit, 10-13 January 2005, Reno, NV, AIAA-2005-1156
- Dawes WN “Towards a fully integrated parallel geometry kernel, mesh generator, flow solver & post-processor”, 44th AIAA Aerospace Sciences Meeting & Exhibit, 9-12 January 2006, Reno, NV, AIAA-2006-45023
- Dawes WN, Harvey SA, Fellows S, Favaretto CF & Vellivelli A “Viscous Layer Meshes from Level Sets on Cartesian Meshes”, 45th AIAA Aerospace Sciences Meeting & Exhibit, 8-11 January 2007, Reno, NV, AIAA-2007-0555
- Dawes WN, Harvey SA, Fellows S, Eccles N, Jaeggi D & Kellar WP “A practical demonstration of scalable, parallel mesh generation” 47th AIAA Aerospace Sciences Meeting & Exhibit, 5-8 January 2009, Orlando, FL, AIAA-2009-0981
- Dawes WN, Harvey SA & Kellar WP “Using Level Sets as the basis for a scalable, parallel geometry engine and mesh generation system” AIAA-2009-0372, Orlando, FL, 2009

Dawes WN, Kellar WK & Richardson GA “Application of topology free optimisation to manage cooled turbine tip heat load” ASME GT2009-59817

Divo E, Steinthorssen E, Rodriguez F, Kassab AJ & Kapat JS “Glenn HT/BEM conjugate heat transfer solver for large scale turbomachinery models” NASA/CR-2003-212195

Dulikravich GS, Denis BH, Martin TJ & Egorov IN “Multi-disciplinary analysis and design optimisation” Invited Lecture, Brazilian Congress on Applied and Computational Mathematics, Bel Horizonte, 2001

Galyean TA & Hughes JF “Sculpting: an interactive volumetric modelling technique” ACM Trans., Computer Graphics, vol.25, no.4, pp 267-274, 1991

Haimes R & Follen GL “Computational Analysis Programming Interface” Proc. 6th Int. Conf. On Numerical Grid Generation in Computational Field Simulations, Eds. Cross, Eiseman, Hauser, Soni & Thompson, July 1998.

Janke E, Hodson HP, Faccini, Popovic I, Lehmann K, Georgakis C, Pons L, Lutum E, Wallin F, Dawes WN & Favaretto F “Selected aerothermal CFD analyses of high pressure turbine topics within the AITEB-2 project”, ECCOMAS-2008, 5th European Congress on Computational Methods in Applied Science and Engineering, Venice-Italy June 30-July 5, 2008

Haller BJ “Transonic turbine cascade” PhD Thesis, Cambridge University, 1979

Lauder B “Wall-function strategies for use in turbulent flow CFD” Computer Modelling/Simulations for Industrial and Environmental Flows, Workshop, Macerata, Italy, October 2007

Legace PA “Unit 4: equations of elasticity”, MIT 16-20, Fall 2002

Li Z & Yang X “An immersed FEM for elasticity equations with interfaces” North Carolina State University, Centre for Research in Scientific Computation, Report, August 2004

Perng K-L, Wang W-T, Flanagan M & Ouhyoung M “A real-time 3D virtual sculpting tool based on modified marching cubes”, SIGGRAPH, 2001

Samareh, JA “Status & Future of Geometry Modelling and Grid Generation of Design and Optimisation” J.of Aircraft, Vol 36, no1, Feb 1999

Tu T, Yi H, Ramirez-Guzman L, Bielak J, Ghattas O, Ma K-L & O’Hallaron DR “From mesh generation to scientific visualization: an end-to-end approach to parallel super-computing” SC2006, Tampa FL, 2006

Verstaete T, Amaral S, van dem Braembussche R Arts T “Design and optimization of the internal cooling channels of a HP turbine blade – Part II, Optimisation” ASME GT2008-51080, Berlin 2008

Viecelli JA “A computing method for incompressible flows bounded by moving walls” J.Comput.Phys, 8, 119-, 1971

Yerry MA & Sheppard MS “Automatic three-dimensional mesh generation by the modified octree technique” Int.J.for Num.Methods in Engineering, vol.20, 1965-1990,1983

-oOo-